15th Australasian Fluid Mechanics Conference
The University of Sydney, Sydney, Australia
13-17 December 2004

Velocity Measurement in Turbulent Boundary Layer of Drag-Reducing Surfactant Solution

M. Itoh[1], S. Tamano[1], K. Yokota[1] and M. Ninagawa[2]

[1]Graduate School of Engineering, Nagoya Institute of Technology, Gokiso-cho, Showa-ku, Nagoya, 466-8555 JAPAN

[2]TOYOTA Motor Corporation, 1 Toyota-cho, Toyota, Aichi 471-8571 JAPAN

Abstract

The influence of a drag-reducing surfactant on a zero pressure gradient turbulent boundary layer was investigated using a two-component laser-Doppler velocimetry (LDV) system. It was found that the streamwise turbulence intensity has an additional maximum near the center of the boundary layer, in addition to the near-wall maximum which appears in the canonical wall-bounded turbulent flow. At the location of the additional maximum, the skewness factor of streamwise turbulent fluctuation is zero.

Introduction

Experimental studies on turbulent channel flow [1, 2, 3] and pipe flow [4, 5, 6] of a drag-reducing surfactant solution have yielded valuable knowledge, such as the stress defect and modification of turbulence structures. On the other hand, there have been no studies on the turbulent boundary layer, which is a typical external flow, of a drag-reducing surfactant solution, while the turbulent boundary layer of a polymer solution was recently investigated [7]. One rheological property of surfactant solutions is that the viscoelastic effect appears only when the shear rate becomes larger than a certain critical value [8]. Therefore, a study of the turbulent boundary layer mixing of the turbulent and potential flows in the surfactant solution will be helpful for understanding the mechanism of drag-reduction, which cannot be obtained by study of the internal flow or the polymer solution.

In the present study, the mean velocity and turbulence statistics were measured using a two-component LDV system in a zero pressure gradient turbulent boundary layer of a drag-reducing surfactant solution. The obtained results were compared with the matching statistics of water.

Experimental Apparatus and Procedure

The experiments were conducted in a closed-loop water tunnel with a cross section of 300 × 300 mm and a length of 1500 mm in which a test plate of 20 × 295 × 1700 mm was installed (see figure 1). A 2-mm diameter trip wire was fixed 100 mm downstream from the leading edge. The difference in free-stream velocities between the location of the leading edge of the test plate and the location 1000 mm downstream was less than 1%. We also confirmed that the freestream turbulence intensity was less than 2%.

The surfactant solution (C_{16}TASal) used here was a mixture of cetyltrimethyl ammonium chloride with sodium salicylate as counterion, which was dissolved in deionized water. The concentration was 75 ppm by weight. The shear viscosity η of the surfactant solution was measured at temperature $T = 20.0\pm0.2^{\circ}$C using a homemade

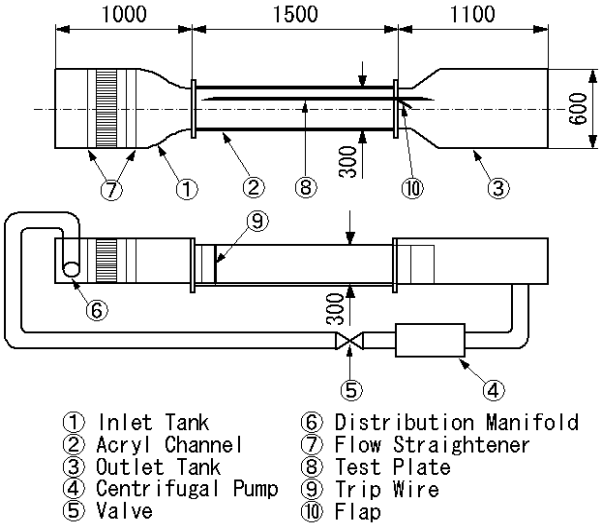

Figure 1: Experimental apparatus

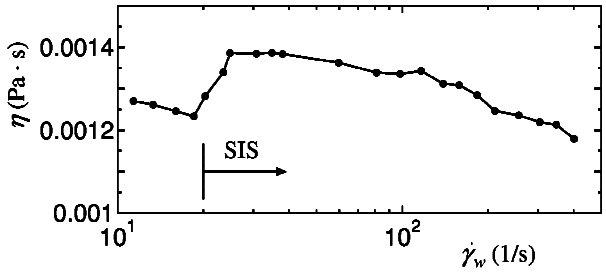

Figure 2: Shear viscosity as a function of the shear rate: C_{16}TASal, 75 ppm, T=20.0^{0}C.

capillary viscometer. Figure 2 shows that the shear viscosity increases suddenly at the shear rate $\dot{\gamma}_w \simeq$ 20 1/s by a factor of about 1.4 compared with that of water, this phenomena is called shear induced state (SIS) [8]. It has been suggested that SIS is strongly related to drag reduction, since in SIS the rod-like micelles form large structures that can directly affect turbulence structures.

The two-component LDV system (300 mW argon-ion laser) was used in back scatter mode. The LDV measurements under the free-stream velocity $U_e \simeq$ 300 mm/s and the fluid temperature $T = 20.0\pm0.1^{\circ}$C were made at the locations downstream from the leading edge x =300, 500, 800 and 1000 mm. The probe was tilted 5° with respect to the test plate surface. The flow was seeded with the nylon powder particles (the mean diameter is 4.1 μm and the specific gravity is 1.02). Typical data rates in the location away from the wall were about 300 Hz, falling off to about 20 Hz very close to the wall. Data samples in the locations away from and near the wall were about 25000 and 5000, respectively.

Table 1: Boundary layer parameters and friction velocity

	C_{16}TASal (75 ppm)				Water			
x (mm)	δ (mm)	δ^* (mm)	θ (mm)	u_τ (mm/s)	δ (mm)	δ^* (mm)	θ (mm)	u_τ (mm/s)
300	12.7	2.91	1.63	13.2	14.8	3.15	2.14	15.3
500	16.8	3.71	2.04	10.6	22.7	3.94	2.72	15.0
800	20.5	4.50	2.47	9.5	29.1	4.82	3.36	14.3
1000	23.0	4.87	2.65	8.5	33.0	5.38	3.78	13.9

Table 2: Non-dimensional parameters of boundary layer

	C_{16}TASal (75 ppm)				Water				
x (mm)	C_f	H	Re_θ	Re_x	C_f	H	Re_θ	Re_x	$\%DR$
300	4.0×10^{-3}	1.788	357	6.58×10^4	5.2×10^{-3}	1.472	641	8.99×10^4	25.6
500	2.5×10^{-3}	1.817	444	1.09×10^5	5.1×10^{-3}	1.451	808	1.49×10^5	50.1
800	2.0×10^{-3}	1.821	535	1.77×10^5	4.6×10^{-3}	1.438	1002	2.38×10^5	55.8
1000	1.6×10^{-3}	1.833	601	2.25×10^5	4.3×10^{-3}	1.425	1136	3.01×10^5	62.6

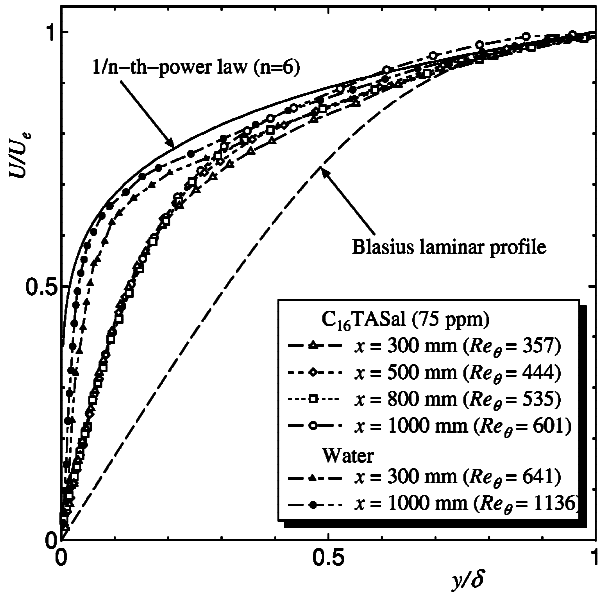

Figure 3: Mean velocity distribution

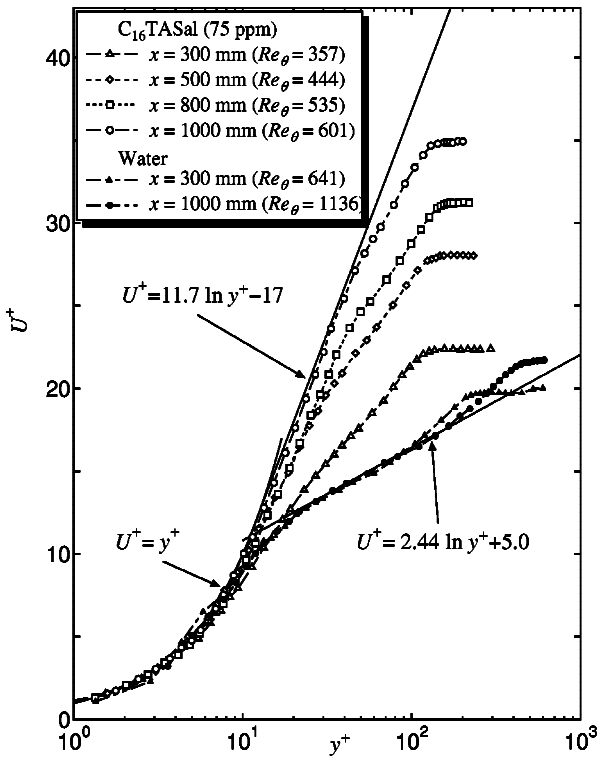

Figure 4: Mean velocity distribution.

Results

Boundary Layer Parameters

The typical boundary layer parameters such as boundary layer thickness δ, displacement thickness δ^* and momentum thickness θ, and the friction velocity u_τ at x =300, 500, 800 and 1000 mm are shown in table 1 for the surfactant solution and water. The friction velocity u_τ was obtained by estimating the wall shear stress from the mean velocity gradient at the wall for the surfactant solution and by the Clauser method for the water, respectively.

As the non-dimensional parameters of the boundary layer, the friction coefficient $C_f = 2(u_\tau/U_e)^2$, shape factor $H = \delta^*/\theta$, momentum-thickness Reynolds number $Re_\theta = U_e\theta/\nu$, where ν it the kinematic viscosity, surface-length Reynolds number $Re_x = U_e x/\nu$, and drag reduction ratio $\%DR$ compared with those of water flow at the same positions and free-stream velocity are shown in table 2. It is found that the shape factor H increases with increasing drag reduction.

Mean Velocity

The distribution of mean velocity scaled by the free-stream velocity is shown in figure 3. The solid and dashed lines in the figure represent 1/n-th-power law (n=6) and the Blasius laminar profile, respectively. The mean velocities U/U_e near the wall ($y/\delta \leq 0.2$) for the surfactant solution, whose profiles are collapsed for the different Reynolds numbers Re_θ, are in about the middle between the mean velocity profile of the water and the Blasius laminar profile.

Figure 4 shows the profiles of mean velocity $U^+ = U/u_\tau$ in the wall-coordinate $y^+ = u_\tau y/\nu$. We confirmed that the measurements for the water agreed well with the corresponding experimental and numerical data [9, 10]. The values of U^+ for the surfactant solution increase with increasing Re_θ, namely increasing the amount of drag reduction. For the surfactant solution at $Re_\theta = 601$, the elastic layer in which the velocity agrees with the Virk's ultimate profile ($U^+ = 11.7\ln y^+ - 17$) [11] exists for $20 < y^+ < 30$, in addition to the standard logarithmic region ($60 < y^+ < 90$). The shear rates $\dot{\gamma}_w$ were about

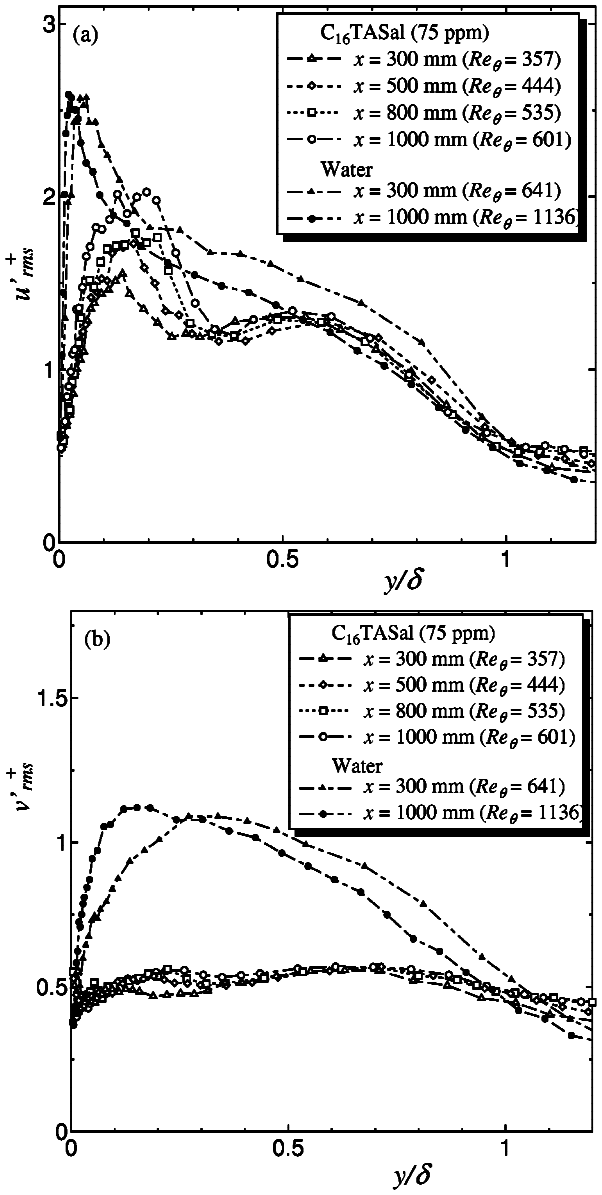

Figure 5: Distribution of turbulence intensity: (a) streamwise, (b) wall-normal

25 and 10 1/s at $y^+ = 30$ and 60, respectively, indicating that the surfactant solutions were in SIS and not in SIS at $y^+ < 30$ and $y^+ > 60$, respectively (see figure 2).

Turbulence Statistics

The distributions of the streamwise and wall-normal turbulence intensities scaled by the friction velocity u'^+_{rms} and v'^+_{rms} are shown in figures 5(a) and 5(b), respectively. The streamwise turbulence intensity u'^+_{rms} of C_{16}TASal increases downstream and is smaller than that of water because of the low-Reynolds number effect, as was also reported in a study on channel flow [1]. It was found that the streamwise turbulence intensity distribution has an additional maximum near the center of the boundary layer, where the solution is not locally in SIS due to the effect of mixing of the potential and turbulent flows, in addition to the standard maximum near the wall. This additional maximum has not been previously observed in the turbulent channel flow [1]. This may be because the large structures of micelles that form near the wall do not disappear suddenly at the center of the channel even

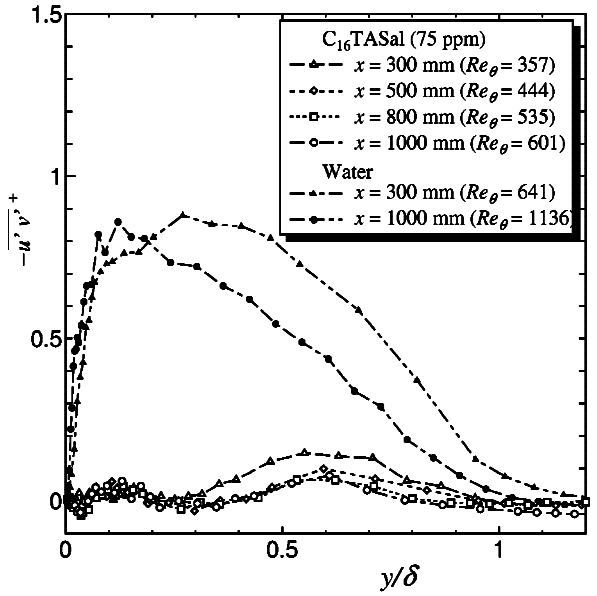

Figure 6: Distribution of Reynolds shear stress

if the shear rate is small there.

The wall-normal turbulence intensity v'^+_{rms} of the surfactant solution is much smaller than that of water and is almost constant across the boundary layer. In addition, the peak of v'^+_{rms} seen in the canonical wall turbulence does not appear.

Figure 6 shows the distributions of the Reynolds shear stress scaled by the friction velocity $-\overline{u'v'}^+$. The Reynolds shear stress of C_{16}TASal, which is much smaller than that of water, has a slight maximum near the center of the boundary layer.

The skewness factors of the streamwise and wall-normal turbulent fluctuations $S_{u'}$ and $S_{v'}$ are shown in figure 7 (a) and figure 7 (b), respectively. The maximum of $S_{u'}$ appears at $y/\delta \simeq 0.5$ for the surfactant solution, as not seen for the water. It is also found that the skewness factor $S_{v'}$ are almost constant ($S_{v'} \simeq 0$) near the outer edge of turbulent boundary layer in the surfactant solution.

Figure 8 shows the distributions of streamwise turbulence intensity u'^+_{rms}, Reynolds shear stress $-\overline{u'v'}^+$, skewness and flatness factors of streamwise velocity fluctuation $S_{u'}$ and $F_{u'}$ for both C_{16}TASal ($Re_\theta = 601$) and water ($Re_\theta = 641$), where dashed lines (a) to (d) represent the locations of $S_{u'} = 0$. For C_{16}TASal, u'^+_{rms} and $F_{u'}$ have the maximum and minimum, respectively, at the location of dashed line (b). This relationship for C_{16}TASal observed at location (b) is qualitatively equal to that of water at location (a). Here the value of y/δ at location (b) is larger than that of location (a), which indicates that the scale of the quasi-streamwise vortex for C_{16}TASal is larger than that for water, as seen in the turbulent channel flow [3]. Note that the relationship between u'^+_{rms} and $F_{u'}$ for C_{16}TASal observed at location (d) is also equal to that of water at location (a).

Conclusions

The influence of a drag-reducing surfactant on a zero pressure gradient turbulent boundary layer was investigated using a two-component LDV system. LDV measurements were made for four different momentum thick-

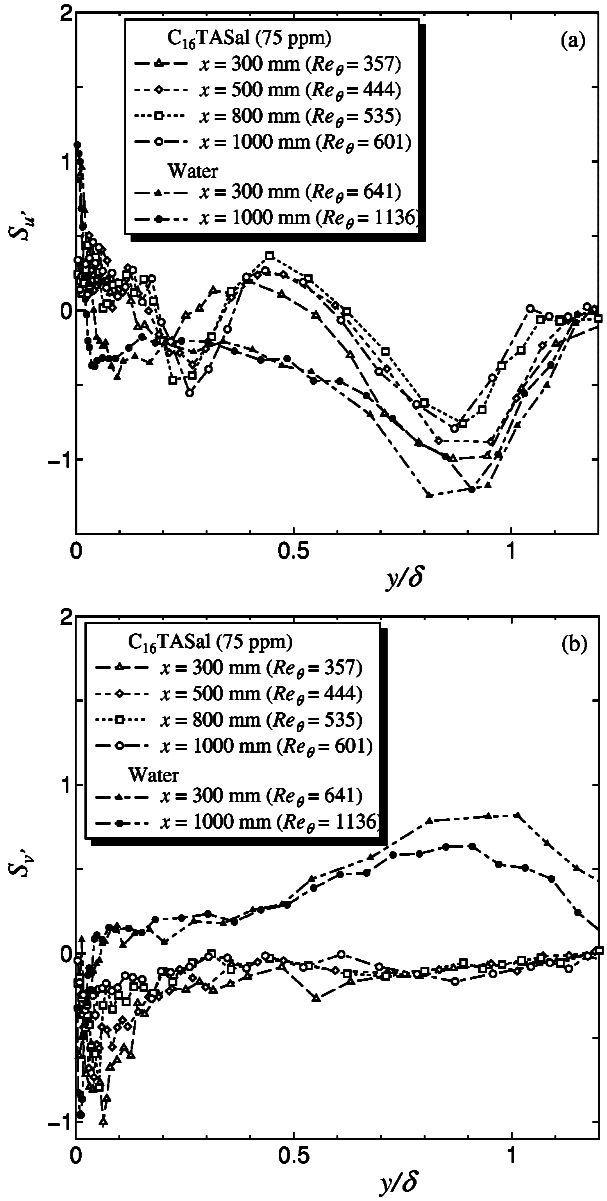

Figure 7: Skewness factor of turbulent fluctuation: (a) streamwise, (b) wall-normal

ness Reynolds numbers, R_θ = 357, 444, 535 and 601. The amount of drag reduction is from 25.6 to 62.6% when compared to a water flow at the same position and free-stream velocity. The mean velocity distribution in wall-coordinates indicates the existence of the elastic layer in addition to the standard logarithmic region. It is found that the streamwise turbulence intensity distribution has the additional maximum near the center of the boundary layer, where the solution is not locally in SIS due to the effect of mixing of the potential and turbulent flows. The location of additional maximum of streamwise turbulence intensity is corresponding to the location at which the skewness factor of streamwise turbulent fluctuation is zero.

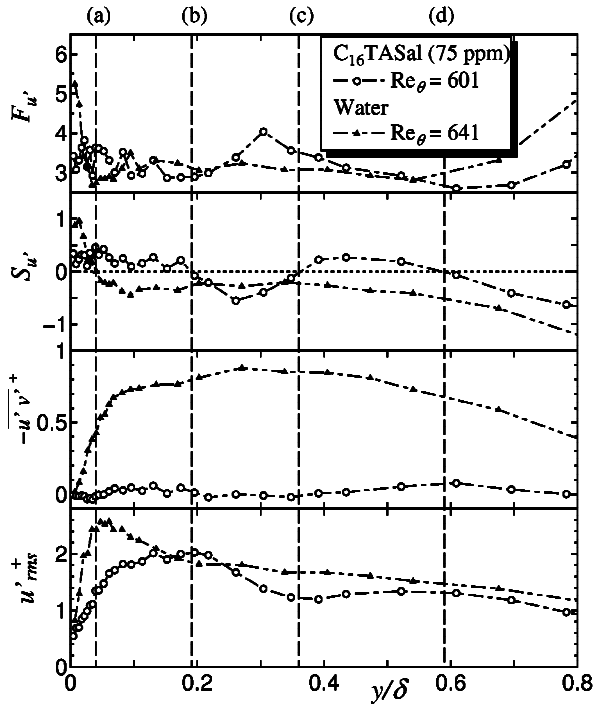

Figure 8: Streamwise turbulence intensity, Reynolds shear stress, skewness and flatness factors of streamwise turbulent fluctuation.

References

[1] Warholic, M.D., Schmidt, G.M. and Hanratty, T.J., The Influence of a Drag-Reducing Surfactant on a Turbulent Velocity Field, *J. Fluid Mech.*, **388**, 1999, 1–20.

[2] Kawaguchi, Y., Segawa, T., Feng, Z. and Li, P., Experimental Study on Drag-Reducing Channel Flow with Surfactant Additives–Spatial Structure of Turbulence Investigated by PIV System, *Int. J. Heat Mass Transfer*, **23**, 2002, 700–709.

[3] Itoh, M. and Kurokawa, Y., Visualization of Turbulent Structure in the Drag-Reducing Flow of Aqueous Surfactant Solution, *Proc. 14th Australasian Fluid Mechanics Conference*, 2001, 877–880.

[4] Chara, Z., Zakin, J.L., Severa, M. and Myska, J., Turbulence Measurements of Drag Reducing Surfactant Systems, *Exp. Fluids*, **16**, 1993, 36–41.

[5] Hetsroni, G., Zakin, J.L. and Mosyak, A., Low-Speed Streak in Drag-Reduced Turbulent Flow, *Phys. Fluids*, **9** (8), 1997, 2397–2404.

[6] Nowak, M., Time-Dependent Drag Reduction and Ageing in Aqueous Solutions of a Cationic Surfactant, *Exp. Fluids*, **34**, 2003, 397–402.

[7] White, C.M., Somandepalli, V.S.R. and Mungal, M.G., The Turbulence Structure of Drag-Reduced Boundary Layer Flow, *Exp. Fluids*, **36**, 2004, 62–69.

[8] Gyr, A. and Bewersdorff, H.-W., *Drag Reduction of Turbulent Flows by Additives*, Kluwer, 1995.

[9] Ching, C.Y., Djenidi, L. and Antonia, A., Low-Reynolds-Number Effects in a Turbulent Boundary Layer, *Exp. Fluids*, **19**, 1995, 61–68.

[10] Spalart, P.R., Direct Simulation of a Turbulent Boundary Layer up to Re_θ = 1410, *J. Fluid Mech.*, **187**, 1988, 61–98.

[11] Virk, P.S., Drag Reduction Fundamentals, *AIChE J.*, **21** (4), 1975, 625–656.